Journal of Hydrology, 137 (1992) 279–310
Elsevier Science Publishers B.V., Amsterdam

[1]

Hydrological modelling of a medium-size mountainous catchment from incomplete meteorological data

Dionysia Panagoulia

Department of Civil Engineering, Division of Water Resources, Hydraulic and Maritime Engineering, National Technical University, Athens, Greece

(Received 20 July 1991; accepted 3 December 1991)

ABSTRACT

Panagoulia, D., 1992. Hydrological modelling of a medium-size mountainous catchment from incomplete meteorological data. J. Hydrol., 137: 279–310.

The US National Weather Service River Forecast System (NWSRFS)-snow accumulation and ablation model, as well as the soil moisture accounting model are developed and tested for purposes of conceptually modelling a medium-size mountainous catchment, i.e. the Mesochora catchment in Central Greece, by using incomplete precipitation and temperature daily records. A combinatorial technique of the Thiessen method and station availability condition, including elevation correction, is adopted for areal and elevation integration of snowmelt model input data. For such an input modelling, the snowmelt model has been proved capable of predicting the initiation of snow accumulation in the fall and the gradual melting of the snowpack in the late winter and spring, while the rainfall–runoff model, which accepts as input the snowmelt model output 'rain plus melt', has also proved capable of accurately reproducing both the magnitude and timing of the annual and monthly runoff. On a daily basis, the runoff model reproduces satisfactorily the historic data, while some discrepancies arise owing to antecedent dry conditions and extreme rainfalls.

INTRODUCTION

The modelling of mountain hydrology is the most challenging object of hydrological simulation, since measurements of meteorological variables in mountainous regions are the most difficult to make and the processes governing mountain hydrology cover the greatest range of demands on theoretical understanding. Regarding the meteorological variables, three major problems are posed: the accessibility to the mountains on a continuous

Correspondence to: D. Panagoulia, Department of Civil Engineering, Division of Water Resources, Hydraulic and Maritime Engineering Technical University, Athens, Greece.

basis, the accuracy of measured meteorological variables, and the areal representativeness of measurements (Klemes, 1990). The problem of accessibility is not connected only to measurements involving water (i.e. rainfall, snow cover and snow water equivalent, etc.), but also to the measurements of surface energy (at least temperature), windspeed and all other phenomena in the boundary layer.

In mountainous areas the accuracy of measured meteorological variables is lower than it is in flat regions. The high slopes and strong wind affect the catch of the true precipitation by the gauges, while harsh conditions cause instruments to malfunction more frequently, thereby leading to gaps in the records, as well as to non-homogeneity, when instruments have to be changed or recalibrated.

Even if measurements could be made where they were necessary and their accuracy could be submitted to control, the problem of their areal representativeness would still remain a formidable obstacle for an accurate description of meteorological variables. The areal representativeness of point measurements is a general and pervasive problem in hydrology, especially in mountainous cases.

The above cited problems are associated with mountain hydrology model inputs. The input modelling from scarce and ineffectively located point measurements of precipitation and energy components, as well as the areal and elevation distribution of precipitation amounts and temperature degrees, represents the most important and elaborate part of a mountain hydrology model (Klemes, 1990).

In this study, the input data of mountain hydrology models are surface- and elevation-wise integrated by introducing a new method which deals with incomplete point records (precipitation and temperature) (Panagoulia, 1991a). A combinatorial technique of the Thiessen method and available station data is proposed. The areal information obtained is corrected for elevation variation. By this double method we can preserve the real nature of meteorological information which is also released from errors that introduce data filling techniques. The aforesaid method can also handle successfully any change in the gauge network, which was the greatest limitation of the classic Thiessen method (Linsley et al., 1988).

As regards the theoretical understanding of the mountain hydrology it includes the disciplines of hydrology, climatology, boundary-layer meteorology, geophysics and geology, as well as the interaction of these processes. The models that simulate the mountain hydrology are the conceptual and direct parameterization ones. While there is much discussion about the intercomparison of snowmelt–runoff models (World Meteorological Organization (WMO) 1986), the deterministic conceptual models, despite the lack of a sounder physical basis, remain attractable for medium-size catchments owing to the detailed hydrological description of the catchment.

The deterministic conceptual models used in this work to simulate the hydrology of a medium-size mountainous catchment, (in this instance the 633 km^2 Mesochora catchment in Central Greece) and which assume as inputs data over area and elevation, integrated with the aforesaid proposed method, are the US National Weather Service River Forecast System (NWSRFS)–snow accumulation and ablation model, and the soil moisture accounting model. The results of this simulation have determined the ability of NWSRFS–soil moisture model to represent the hydrological dynamics of a medium-size catchment during dry to wet transitions and extreme rainfall. Some new findings have been extracted that bear several similarities with findings of Gan and Burges (1990a, b) for small hypothetical catchments. These findings indicate also that special attention must be given to the choice of the time horizon of hydrological response analysis to climate change, when the US NWSRFS models are used (Panagoulia, 1990).

CATCHMENT FEATURES AND CLIMATE

The Mesochora catchment (632.8 km^2, Fig. 1) lies in the central mountain region of Greece and extends nearly 32 km from north (39° 42′) to south (39° 25′) with an average width of about 20 km. The Pindus Mountains, with peak elevations of about 2300 m, form the western boundary of the catchment, while the eastern one is formed by the Koziakas mountains with peaks of about 2000 m. Inside, the catchment presents intense topography with strong interchanges of lower and higher elevations. The mean elevation of catchment is 1390 m. The wild Acheloos river traverses the catchment formed by a number of lower and higher order streams.

The climate in the Mesochora catchment is elevation-dependent, with hot summers and mild winters at low elevations and mild summers and cold winters at high elevations. Because of its high mean elevation, its hydrology is controlled by snowfall and snowmelt. The mean annual precipitation of the catchment (weighted average over elevation bands) is about 1898 mm, and most of the precipitation falls as snow at the higher elevations. The mean annual runoff of the catchment is about 1170 mm (or 23.5 $m^3 s^{-1}$). The mean January and July daily temperatures (weighted average over elevation bands) are.

Mean January daily temperature (°C)			Mean July daily temperature (°C)		
Daily average	Minimum	Maximum	Daily average	Minimum	Maximum
0.10	−3.51	3.71	17.53	11.43	23.63

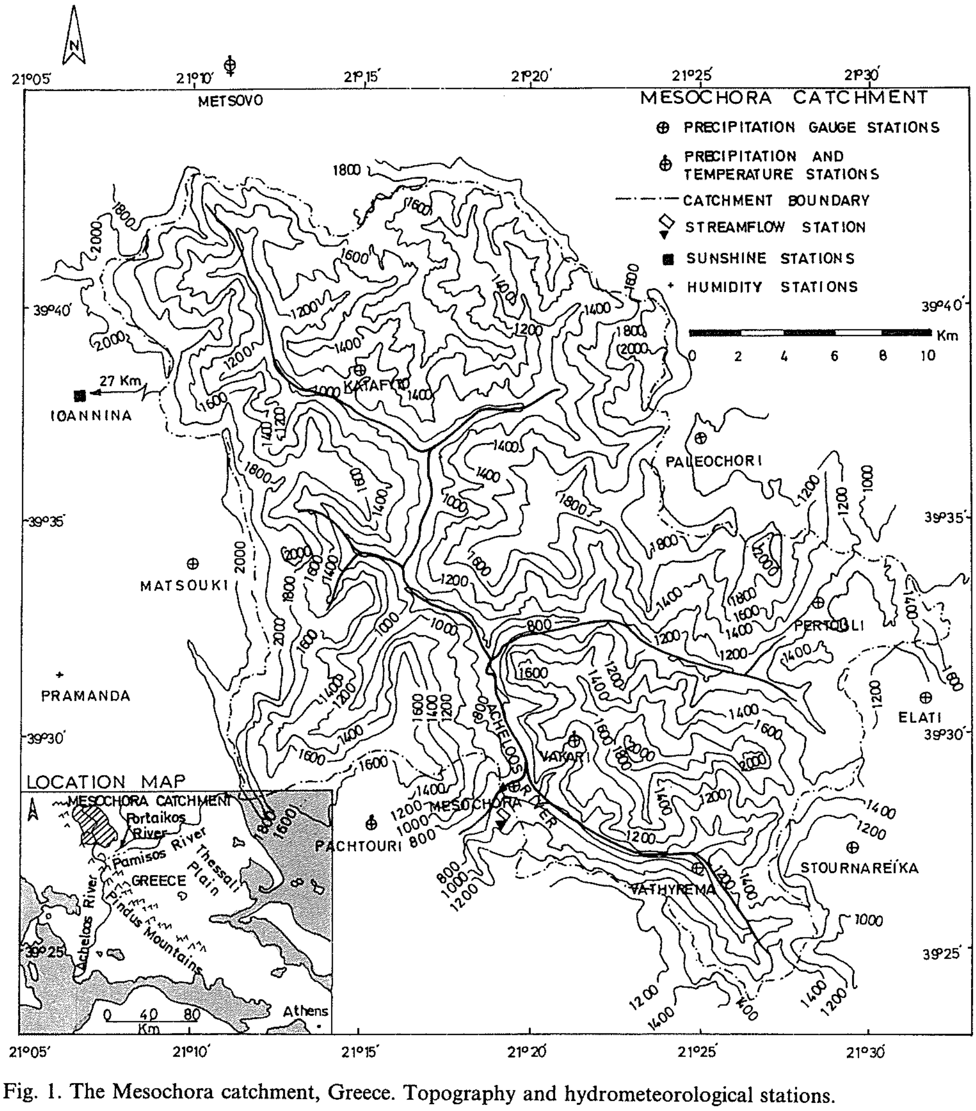

Fig. 1. The Mesochora catchment, Greece. Topography and hydrometeorological stations.

The soils of the catchment have been formed from decay of hard limestones and flysch. They are varied, but generally permeable.

Mesochora, which constitutes the upper drainage catchment of Acheloos river, has a great significance for Greece because the river will be partially diverted at the outfall of the Mesochora catchment through the Pindus mountains to irrigate the arid Thessaly Plain. It is the largest construction project for Greece, including five dams (one is Mesochora's), 24 miles of large tunnels and about 5000 miles of buried irrigation pipes.

DETERMINISTIC CONCEPTUAL MODELS: THE US NWSRFS SNOWMELT AND RAINFALL–RUNOFF MODELS

The hydrology of a catchment from precipitation to stream discharge at the lowest outfall, can be conceived as a series of interlinked processes and storages. In conceptual simulation, the catchment processes are described mathematically, and the storages are considered as reservoirs, for which water budgets are kept (Shaw, 1984).

Many conceptual catchment models have been developed over the last two decades (e.g. Stanford IV (Crawford and Linsley, 1966), SSARR (Schermerhorn and Kuehl, 1968), USDAHL-74 (US Agricultural Research Service, 1975), DISPRIN (Jamienson and Wilkinson, 1972), etc.), each one structured by different combinations of processes, storages and interchanges, and each requiring some specific sets of input data.

Most of these models are deterministic (the modelled processes do not include a stochastic part) and operate on discrete time segments related to a precipitation event (event models), or operate continuously for moisture accounting storage and release regardless of precipitation events (continuous models).

Others of these models are classified as lumped parameter models and some others as distributed ones. The lumped parameter models rely on the fact that the spatial variability of governing parameters is 'lumped' to form an 'effective value', which is applied to the entire catchment (Huggins and Burney, 1982), while the distributed models incorporate spatial variability of parameters directly in the model formulation through partial differential equations, which describe system behaviour with an infinite set of boundary conditions (Huggins and Burney, 1982).

Given that there is a relatively large number of conceptual models, the problem of choice of the best one comes up. The required information for such a choice, in first level, includes time step of model operation, model availability and purpose of model use, as well as modelled process and basin size, plus data and temporal resolution of input and output of model. It is evident from the above information that more than one model can simulate successfully the same catchment. For this reason, the selection problem of the optimum model is resolved in a second level, based on the following criteria (Linsley, 1982; James and Burges, 1982; Woolhiser and Brakensiek, 1982; James et al., 1982): (1) accuracy of prediction; (2) ease of use; (3) applicability to the problem; (4) generality of implementation; (5) consistency in parameter estimation; (6) sensitivity of model results to changes in parameters and input variables. However, there is not any better model.

Although the conceptual watershed models require various sets of data and much computation time for their parameters' calibration, said models are nonetheless widely used, not only to simulate the entire behaviour of the catchment, but to investigate the interaction of the hydrometeorological variables among them, i.e. the influence of temperature, rainfall, etc. on runoff (WMO, 1975). Thus the US National Weather Service models of snow accumulation and ablation, as well as the soil moisture accounting, have been selected for the purposes of this study. Both models are the most representative types of deterministic conceptual models. They also are well documented and have been widely used, the first for snow accumulation and snowmelt, the second for streamflow simulation and forecasting.

Snow accumulation and ablation model

This model was developed by Eric Anderson within the US National Weather Service Hydrologic Research Laboratory (Anderson, 1973). This is a deterministic, conceptual model consisting of a set of equations which describe the accumulation and ablation of a snowpack. The model inputs are air temperature and precipitation at a 6 hourly time step. In this study, daily precipitation was interpolated to 6 hourly increments and 6 hourly temperature was estimated from daily temperature maxima and minima using equations furnished by Anderson.

The model can be summarized as follows. Accumulation of snowpack occurs when air temperature, T_a, is less than the delineation temperature which can be 0°C or other. In the opposite case ($T_a >$ delineation temperature) the model assumes that the precipitation is rain. The ablation of snowpack is controlled by the heat exchange at the air-snow interface. For heat exchange computations there are two basic conditions (1) when the air is warm ($T_a > 0$°C) in which case melt takes place at the snow surface, and (2) when the air is too cold ($T_a < 0$°C) for melt to occur. Furthermore, the melt is computed for rain or non-rain periods. For melt during rain periods the following assumptions are made: (1) there is no solar radiation; (2) incoming longwave radiation is equivalent to blackbody longwave radiation at T_a; (3) snow surface temperature is 0°C; (4) the dew point is T_a; and (5) the rain temperature is T_a. Under these assumptions, the amount of melting snowpack expressed as heat losses ΔQ is: $\Delta Q = Q_n + Q_e + Q_h + Q_{px}$, where Q_n = long wave radiation, Q_e = latent heat transfer due to condensation, Q_h = sensible heat transfer, and Q_{px} = heat transfer by rain water.

For melt during non-rain periods, the model checks whether the snowpack is isothermal at 0°C. If the snowpack is not isothermal, no melt occurs and the net heat flux is added to the heat content of the snowpack. If the snowpack is isothermal, and the air temperature is $T_a > 0$°C, melt occurs at a rate proportionate to a seasonally varying melt factor and the difference between the air temperature and 0°C.

During non-melt periods (the model assumes $T_a < 0$°C), an antecedent temperature index, (ATI), is used as an index to the temperature of the surface layer of snowpack. The heat exchange is assumed proportional to the temperature gradient defined by current air temperature and the antecedent temperature index. The proportionality constant is a parameter 'called the negative melt factor' which varies seasonally in the same way as does the melt factor used during non-rain periods.

The model accounts for the areal extent of snow cover. During the periods of snow accumulation, this is assumed to be 100%. During periods of depletion, the model uses an areal depletion curve of snow, that is a function of the areal extent of snow cover versus the ratio of mean areal water equivalent to an index value, which is the smaller of the maximum water equivalent (since snow began to accumulate), or a preset maximum. The six major and six minor parameters of the snow model are described in the section of parameter estimation.

Soil moisture accounting model

The model was developed by Burnash et al. (1973) and forms the basis of the US National Weather Service's basic catchment hydrologic response model for operational forecasting. It is a deterministic, continuous, lumped-parameter, conceptual model. The original model was designed for daily precipitation input but later versions allow finer time increments (6 h or less). Input to the model is pseudoprecipitation (rain plus melt model output) and potential evaporation (actual, or long-term average). The model is based on a system of percolation, soil moisture storage, drainage and evapotranspiration characteristics to represent the significant hydrologic process in a rational manner.

Figure 2 shows the components of the soil moisture hydrological model. As seen from this figure, the model is represented by an upper and lower zone. The upper zone is divided into tension water storage and free water storage for the permeable portion of the catchment. Tension water is considered as that water which is closely bound to soil particles. This water is available for

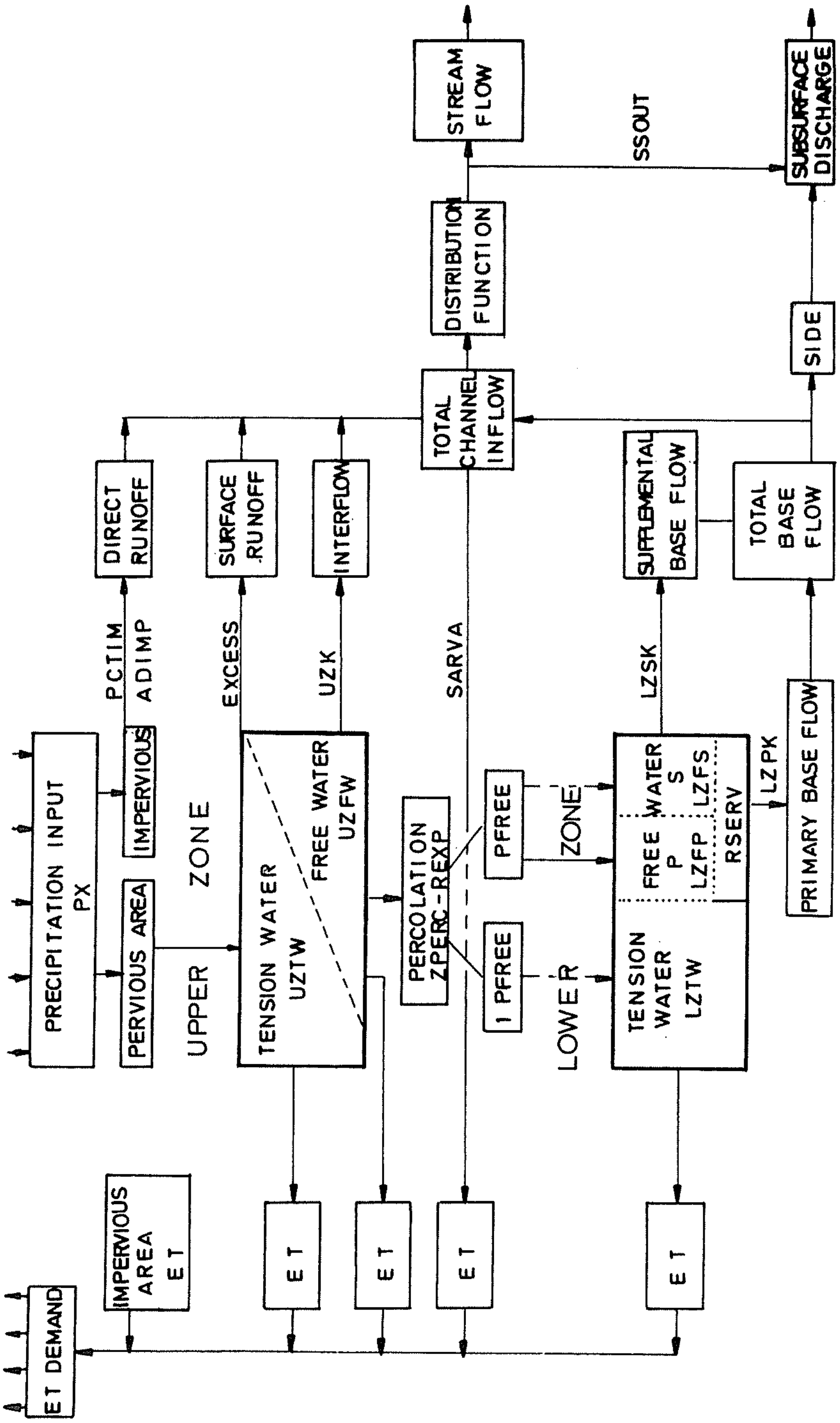

Fig. 2. Soil moisture accounting model components.

evapotranspiration based on the upper zone soil moisture. Tension water storage should be filled up before moisture becomes available to enter the free water storage. Free water can descend to a lower zone by percolation or can move laterally to produce interflow. Percolation is controlled by the contents of the upper zone free water and the deficiency of lower zone moisture volume. When the precipitation rate exceeds the percolation rate and the maximum interflow drainage capacity, then the upper zone free water capacity is filled completely and the excess rainfall will result in surface runoff.

Lower zone consists of tension water storage and two free water storages. Again, the tension water is available for evapotranspiration. The two free water storages fill simultaneously from percolated water and drain independently at different rate, giving a variable ground water recession. Direct runoff from impervious area, surface runoff, interflow and base flow from lower zone contribute to generate the channel inflow.

The model employs about 21 parameters. These are soil moisture storage parameters for upper and lower zone, percolation parameters, catchment characteristics, etc. These parameters are described in the section of parameter estimation. Some parameters can be estimated from semi-log plot of discharge or geographic maps of the study area.

INPUT DATA

Three categories of stations and data, according to their use by the models, are described. These are: (1) precipitation and temperature stations with daily data; (2) temperature, sunshine, and humidity stations with monthly data; (3) streamflow station with daily data.

In addition, the methods used to average the station measurements data over area and elevation are described.

Precipitation and temperature stations-data

Eleven precipitation stations are installed within and around the Meschora catchment, with the greater density at the lower part of the catchment (Fig. 1). The general characteristics of the stations for the study period (1972–1986) are presented in Table 1.

The precipitation stations are consistent and representative of the catchment, but in some precipitation records daily data are missing. We did not interpolate them for three reasons: (1) in order to preserve the real nature of precipitation-temperature series elements; (2) in order to avoid the computing errors that are introduced by the estimation techniques of daily missing data (Linsley et al., 1988); (3) because these last techniques are applied with difficulty (e.g. the application of multisite stochastic models). Thus, the

TABLE 1

Precipitation gauge stations by elevation zone, and temperature stations for the entire Mesochora catchment (catchment area = 632.8 km^2)

Zone	Stations	Station elevation (m)	Zone elevation range (m)	Zone median elevation (m)	Zone area (%)	Years of record: Precipitation	Years of record: Temperature max	Years of record: Temperature min
Upper	Metsovo	1157				15	14	15
	Katafyto	980	1580–2200	1830	30.54	15		
	Palaiochori	1050				15		
Middle	Palaiochori	1050				15		
	Matsouki	1079	1280–1580	1400	29.51	15		
	Pertouli	1160				15		
Lower	Tyrna (elati)	900				15		
	Vakari	1150				15	15	15
	Mesochora	780				15		
	Pachtouri	950	780–1280	1080	39.95	15	11	11
	Stournareika	860				15		
	Vathyrema	920				15		

technique used to estimate the mean areal daily precipitation was a combinatorial one of the Thiessen method and station daily availability, including elevation correction (Panagoulia, 1991a). The correction areal precipitation factor for a given elevation (e.g. midpoint catchment elevation) is obtained from the following algorithm.

$$p_e = \frac{P + (e - e_{ws})p_f}{P} \quad (1)$$

where p_e is the multiplying corrective precipitation factor for elevation e, P is the mean areal precipitation, e_{ws} is the weighted mean station elevation based on station daily availability, and p_f is the variation rate of precipitation with elevation.

As regards the network of temperature stations there are three stations. One is installed inside the catchment, while the other two are installed outside and present significant deficiencies of daily maximum and minimum data. The consistency of the data was checked by the double-mass curve on a monthly basis (Anderson, 1973), and some deviations from a straight line were observed for minimum data. The inconsistent data were corrected by applying an appropriate corrective factor of the order -0.6 to -1.0°C. For the implementation of consistency checking only, if there were missing monthly

TABLE 2

Sunshine, temperature, and humidity gauge stations of Mesochora catchment

Meteorological variable	Stations	Station elevation (m)	Period of records
Sunshine	Ioannina	483	1972–1986
	M. Kerasia	560	1972–1986
Temperature	Metsovo	1156	1961–1986
	Vakari	1150	1972–1986
	Pachtouri	950	1972–1981
Humidity	Metsovo	1156	1970–1986
	Pramanta	835	1970–1986

minimum temperatures, these were interpolated by the long-term average values of their existing monthly data. The consistency checking of the corrected actual data did not show an absolute straight line in the double-mass curve diagram, but two or three hardly distinguishable parallel straight-lines.

The technique used to estimate the mean areal maximum and minimum daily temperature was also a combinatorial technique of the Thiessen method and station daily availability.

The correction areal temperature factor for a given elevation is obtained from the following algorithm:

$$T_e = (e - e_{ws})T_f \qquad (2)$$

where, T_e is the additive corrective temperature factor for elevation e, e_{ws} is the weighted mean station elevation based on station daily availability, and T_f is the rate of temperature decrease with elevation (lapse rate).

Potential evapotranspiration

In order to obtain the catchment potential evapotranspiration, the sunshine, temperature and humidity data were considered. Their measurement stations are described in Table 2. The sunshine stations are outside the catchment, the Ioannina is at the northwest boundary of the catchment, while the M. Kerasia station is at the eastern boundary. The catchment sunshine is computed from the long-term monthly arithmetic average of the sunshine of the two stations. As shown above, the catchment humidity from the two stations was also calculated. The Pramanta station is installed outside the catchment near the western boundary.

The catchment temperature was estimated using the above Thiessen method combining it with the monthly station availability. The areal temperature was corrected for catchment mean elevation by applying a monthly dependent lapse rate according to eqn. (2). The long-term monthly mean catchment sunshine, temperature, and humidity were used as inputs to the Penman equation which is given in Veihmeyer (1964) to estimate the catchment potential evapotranspiration.

Other inputs to the Penman equation were the average wind speed, (200 miles day^{-1}), the monthly percent of reflecting surface and the solar radiation for the midpoint catchment latitude. The sunshine was entered to the Penman equation as monthly ratio of duration of bright sunshine to maximum possible duration of bright sunshine.

Streamflow

The daily streamflow data of the Mesochora gauge station for the period 1972–1986, were used in this study. Most of the streamflow records were complete, but some missing daily data were included. For estimating the missing data, the Avlaki station was used as a backup station, while the average monthly streamflow for both stations was computed. The Mesochora missing data were estimated by multiplying the complete daily data of the Avlaki station by the ratio of the monthly average streamflow (Mesochora/Avlaki).

MODEL CALIBRATION

The procedures used for model calibration (parameter estimation) and soil moisture accounting model validation and verification are developed as follows.

Snow accumulation and ablation model parameter estimation

The mountainous catchment was divided into elevation zones, and the snowmelt model was applied to each zone separately, since low elevations are likely to receive rain, while higher elevations receive snow from the same storm. The weighted mean value of the pseudo-precipitation from all zones was treated as the mean areal precipitation which is the input to the soil-moisture accounting model. In general, the weighting factors used were equal to the ratios of the elevation zone subareas for the total catchment area.

The elevation bands were delineated as follows: first a hypsometric curve (elevation versus area fraction) was developed. The catchment was then divided into three zones of area, depending on the elevation range, and the elevation of the midpoint of each band was identified (Table 1).

The snowmelt model was manually calibrated for the three elevation zones. According to available station data on that particular day, for every elevation zone, the precipitation–elevation correction factors p_e, were estimated through a trial and error approach, which was carried out concurrently with the calibration of the soil moisture accounting model. The final precipitation–elevation correction factors are given in Table 3.

As with the function p_e, the lapse rate is usually non-linear. It was found that average lapse rates for four periods (each 6 h long) of each day is −0.80°C per 100 m. The lapse rates, T_f and the temperature correction factors, T_e, were also estimated concurrently with the calibration of the soil moisture model, and their final values are given in Table 4.

Seasonal melt factors were interpolated between MFMAX and MFMIN and were estimated to 0.9 and 0.4 mm°C^{-1} per 6 h, respectively. PXTEMP, the temperature (°C) above which precipitation was assumed to be rain was assumed to be 1°C for the first 6 months of the calendar year, and 0°C for the rest. The mean areal water-equivalent (SI) above which 100% areal snow cover always exists, was assumed to be 100 mm. The depletion snow curve was formed from the pairs of the following values:

Areal mean water-equivalent/Ai:	0.0	0.1	0.2	0.3	0.4	0.5	0.6	0.7	0.8	0.9	1.0
Snow cover extent :	.05	.11	.18	.20	.22	.25	.33	.42	0.53	0.71	1.00

Description and calibrated values of the snow-melt model parameters are shown in Table 5.

Soil moisture accounting model parameter estimation

Parameter estimation for the soil moisture accounting model was based on a process of initial parameter estimation, as suggested by Peck (1976). The final values of parameters were obtained by the manual model calibration on the Mesochora catchment. The description of model parameters and their final values are listed in Table 6. The model was calibrated for the whole study period from 1972 to 1986, which included dry, medium and wet years, so that the model could be subjected to a broad range of changes in conceptual storages.

The results of error analysis of daily flow, as well as the 3 day volume error analysis including peaks, are presented in Tables 7 and 8, respectively. The values taken from the statistic parameters of Table 7, as well as the comparison between simulated and observed flow components of Table 8, suggest that both hydrological models were proved capable of reproducing

TABLE 3

Station weights and precipitation correction factors

No.	Availability station	Lower zone						$p_f = 0.02$ p_e
		Tyrna	Vakari	Mesochora	Pachtouri	Stournar	Vathyrema	
1	000001	0.00000	0.00000	0.00000	0.00000	0.00000	1.00000	1.00171
2	000010	0.00000	0.00000	0.00000	0.00000	1.00000	0.00000	1.00236
3	000011	0.00000	0.00000	0.00000	0.00000	0.16123	0.83877	1.00182
4	000100	0.00000	0.00000	0.00000	1.00000	0.00000	0.00000	1.00139
5	000101	0.00000	0.00000	0.00000	0.37290	0.00000	0.62710	1.00160
6	000110	0.00000	0.00000	0.00000	0.49258	0.50742	0.00000	1.00188
7	000111	0.00000	0.00000	0.00000	0.37290	0.16123	0.46587	1.00170
8	001000	0.00000	0.00000	1.00000	0.00000	0.00000	0.00000	1.00322
9	001001	0.00000	0.00000	0.53907	0.00000	0.00000	0.46093	1.00252
10	001010	0.00000	0.00000	0.63996	0.00000	0.36004	0.00000	1.00291
11	001011	0.00000	0.00000	0.53907	0.00000	0.16123	0.29970	1.00263
12	001100	0.00000	0.00000	0.80020	0.19980	0.00000	0.00000	1.00285
13	001101	0.00000	0.00000	0.33927	0.19980	0.00000	0.46093	1.00216
14	001110	0.00000	0.00000	0.44016	0.19980	0.36004	0.00000	1.00254
15	001111	0.00000	0.00000	0.33927	0.19980	0.16123	0.29970	1.00226
16	010000	0.00000	1.00000	0.00000	0.00000	0.00000	0.00000	0.99925
17	010001	0.00000	0.64194	0.00000	0.00000	0.00000	0.35806	1.00013
18	010010	0.00000	0.71315	0.00000	0.00000	0.28684	0.00000	1.00014
19	010011	0.00000	0.62908	0.00000	0.00000	0.15232	0.21859	1.00026
20	010100	0.00000	0.76558	0.00000	0.23442	0.00000	0.00000	0.99975
21	010101	0.00000	0.40752	0.00000	0.23442	0.00000	0.35806	1.00064
22	010110	0.00000	0.47873	0.00000	0.23442	0.28684	0.00000	1.00064
23	010111	0.00000	0.39466	0.00000	0.23442	0.15232	0.21859	1.00076
24	011000	0.00000	0.65480	0.34520	0.00000	0.00000	0.00000	1.00062
25	011001	0.00000	0.29871	0.34323	0.00000	0.00000	0.35806	1.00149

26	011010	0.00000	0.36795	0.34520	0.00000	0.28684	0.00000	1.00151
27	011011	0.00000	0.28586	0.34323	0.00000	0.15232	0.21859	1.00162
28	011100	0.00000	0.65480	0.14540	0.19980	0.00000	0.00000	1.00025
29	011101	0.00000	0.29871	0.14342	0.19980	0.00000	0.35806	1.00113
30	011110	0.00000	0.36795	0.14540	0.19980	0.28684	0.00000	1.00115
31	011111	0.00000	0.28586	0.14342	0.19980	0.15232	0.21859	1.00126
32	100000	1.00000	0.00000	0.00000	0.00000	0.00000	0.00000	1.00193
33	100001	0.13947	0.00000	0.00000	0.00000	0.00000	0.86053	1.00174
34	100010	0.14342	0.00000	0.00000	0.00000	0.85658	0.00000	1.00230
35	100011	0.11573	0.00000	0.00000	0.00000	0.06034	0.82394	1.00178
36	100100	0.43719	0.00000	0.00000	0.56281	0.00000	0.00000	1.00163
37	100101	0.13947	0.00000	0.00000	0.37290	0.00000	0.48764	1.00162
38	100110	0.14243	0.00000	0.00000	0.49258	0.36498	0.00000	1.00182
39	100111	0.11573	0.00000	0.00000	0.37290	0.06034	0.45104	1.00166
40	101000	0.25519	0.00000	0.74481	0.00000	0.00000	0.00000	1.00289
41	101001	0.13947	0.00000	0.53907	0.00000	0.00000	0.32146	1.00255
42	101010	0.12463	0.00000	0.63403	0.00000	0.24135	0.00000	1.00285
43	101011	0.11573	0.00000	0.53907	0.00000	0.06034	0.28487	1.00259
44	101100	0.25519	0.00000	0.54501	0.19980	0.00000	0.00000	1.00252
45	101101	0.13947	0.00000	0.33927	0.19980	0.00000	0.32146	1.00219
46	101110	0.12463	0.00000	0.43422	0.19980	0.24135	0.00000	1.00248
47	101111	0.11573	0.00000	0.33927	0.19980	0.06034	0.28487	1.00222
48	110000	0.17310	0.82690	0.00000	0.00000	0.00000	0.00000	0.99971
49	110001	0.12760	0.61721	0.00000	0.00000	0.00000	0.25519	1.00022
50	110010	0.10386	0.70129	0.00000	0.00000	0.19486	0.00000	1.00013
51	110011	0.10386	0.61721	0.00000	0.00000	0.06034	0.21859	1.00025
52	110100	0.17310	0.59248	0.00000	0.23442	0.00000	0.00000	1.00022
53	110101	0.12760	0.38279	0.00000	0.23442	0.00000	0.25519	1.00072
54	110110	0.10386	0.46686	0.00000	0.23442	0.19486	0.00000	1.00064
55	110111	0.10386	0.38279	0.00000	0.23442	0.06034	0.21859	1.00076
56	111000	0.17310	0.48170	0.34520	0.00000	0.00000	0.00000	1.00108
57	111001	0.12760	0.27399	0.34323	0.00000	0.00000	0.25519	1.00158
58	111010	0.10386	0.35608	0.34520	0.00000	0.19486	0.00000	1.00150

TABLE 3

(Continued)

No.	Availability station	Lower zone						$p_f = 0.02$
		Tyrna	Vakari	Mesochora	Pachtouri	Stournar	Vathyrema	p_e
59	111011	0.10386	0.27399	0.34323	0.00000	0.06034	0.21859	1.00162
60	111100	0.17310	0.48170	0.14540	0.19980	0.00000	0.00000	1.00072
61	111101	0.12760	0.27399	0.14342	0.19980	0.00000	0.25519	1.00122
62	111110	0.10386	0.35608	0.14540	0.19980	0.19486	0.00000	1.00114
63	111111	0.10386	0.27399	0.14342	0.19980	0.06034	0.21859	1.00125

No.	Availability station	Middle zone			$p_f = 1.20$
		Palaiochor	Matsouki	Pertouli	p_e
1	001	0.00000	0.00000	1.00000	1.18637
2	010	0.00000	1.00000	0.00000	1.24927
3	011	0.00000	0.52075	0.47925	1.21913
4	100	1.00000	0.00000	0.00000	1.27180
5	101	0.83266	0.00000	0.16734	1.25750
6	110	0.59706	0.40295	0.00000	1.26272
7	111	0.42972	0.40295	0.16734	1.24843

No.	Availability station	Upper zone			$p_f = 0.63$
		Metsovo	Katafyto	Palaiochor	p_e
1	001	0.00000	0.00000	1.00000	1.34795
2	010	0.00000	1.00000	0.00000	1.37918
3	011	0.00000	0.84864	0.15136	1.37445
4	100	1.00000,	0.00000	0.00000	1.30022
5	101	0.58603	0.00000	0.41397	1.31998
6	110	0.10737	0.89263	0.00000	1.37070
7	111	0.10737	0.74127	0.15136	1.36597

TABLE 4

Station weights and zone temperature correction factors T_c for lapse rate $T_r = -0.80$

No.	Availability station	Station			Zone		
		Metsovo	Vakari	Pachtouri	Upper	Middle	Lower
1	001	0.00000	0.00000	1.00000	−7.04000	−3.60000	−1.04000
2	010	0.00000	1.00000	0.00000	−5.44000	−2.00000	0.56000
3	011	0.00000	0.73449	0.26551	−5.86481	−2.42481	0.13519
4	100	1.00000	0.00000	0.00000	−5.39200	−1.95200	0.60800
5	101	0.30423	0.00000	0.69577	−6.53863	−3.09863	−0.53863
6	110	0.26393	0.73607	0.00000	−5.42733	−1.98733	0.57267
7	111	0.25840	0.58238	0.15923	−5.68236	−2.24236	0.31764

the observed streamflow (the snowmelt model indirectly, and the rainfall–runoff model directly). Also, the typical monthly simulation errors expressed in percent of observed flows, were of the order of 10–15%, higher in low runoff months (August and September) and lower in high runoff months. A

TABLE 5

Snow melt model parameter description and parameter calibrated values

Parameter	Description	Calibrated values
SCF	A multiplying factor to correct for gauge catch deficiency in the case of snowfall	1.10
MFMAX	Maximum melt factor during non-rain periods which occurs on June 21 (mm °C^{-1} per 6 h)	0.90
MFMIN	Minimum melt factor during non-rain periods which occurs on December 21 (mm °C^{-1} per 6 h)	0.40
UADJ	Average wind function during rain on snow periods (mm mb^{-1} per 6 h)	0.10
SI	Mean areal water-equivalent above which there is always 100% areal snow cover (mm)	100
NMF	Maximum negative melt factor (mm$_e$ °C^{-1} per 6 h)	0.12
TIMP	Antecedent temperature index parameter	0.30
PXTEMP	Temperature which delineates rain from snow (°C)	1.0–0
MBASE	Base temperature for snow melt computation during non-rain periods (°C)	0
PLWHC	Percent liquid-water holding capacity of ripe snow	0.05
PAYGM	Average daily ground at the snow-soil interface (mm)	0.020
EFC	Percent area over which evapotranspiration occurs when there is 100% snow cover	0.61

TABLE 6

Soil moisture accounting model parameter description and parameter final values

Soil moisture phase	Parameters	Description	Final values
Direct runoff	PCTIM	Minimum impervious catchment (%)	0.01
	ADIMP	Additional impervious catchment (%)	0.01
	SARVA	Catchment covered by streams, lakes and riparian vegetation (%)	0.0
Upper zone	UZTWM	Upper zone tension under capactiy (cm)	4.50
	UZFWM	Upper zone free water capacity (cm)	4.61
	UZK	Daily upper zone free water drainage rate	0.57
Percolation	ZPERC	Proportional increase in percolation from saturated to dry condition	6.00
	REXP	Exponent affecting rate of change of percolation between wet and dry conditions	1.80
Lower zone	LZTWM	Lower zone tension water capacity (cm)	25.00
	LZFSM	Lower zone supplementary free water capacity (cm)	9.00
	LZFPM	Lower zone primary free water capacity (cm)	30.00
	LZSK	Daily lower zone supplementary free water drainage rate	0.15
	LZPK	Daily lower zone primary free water drainage rate	0.015
	PFREE	Percolation water fraction passing directly to lower zones free water	0.20
	RSERV	Fraction of lower zone free water unavailable for transpiration	0.10
	SIDE	Ratio of non-channel baseflow to channel baseflow	0.00
Initial water	UZTWC	Upper zone tension water content (cm)	4.50
	UZFWC	Upper zone free water content (cm)	0.11
	LZTWC	Lower zone tension water content (cm)	21.41
	LZFSC	Lower zone supplementary free water content (cm)	0.088
	LZFPC	Lower zone primary free water content (cm)	2.26
	ADIMC	Tension water content of the additional impervious catchment (cm)	25.91

TABLE 7

Error analysis of daily runoff

Runoff ($m^3 s^{-1} km^2$)	Total	Surface	Upper level	Lower level
Standard error	0.53	0.76	0.66	0.47
Average bias	0.017	0.525	0.134	−0.056
Days	5479	491	608	4380
Mean discharge	3.70	11.12	8.00	2.37

Standard error of daily mean flow 3 $m^3 s^{-1}$

more detailed comparison of the soil moisture accounting model with actual runoff conditions is presented below.

Model validation

While there are many criteria for describing how well a particular model performs the task for which it was employed (i.e. criteria cited in the above section, root mean square error, coefficient of efficiency, etc.), we selected a graphical display (time series plot) to show some particular differences between simulated and observed daily runoff series that are probably hidden in summarized daily flow error analysis or in monthly flow error analysis.

Although the proposed integration precipitation and temperature method is free from computing errors of entering data, we cannot exclude that these discrepancies might be due to rainfall simulation problems. On the other hand, the discussed differences are compatible with those of Gan and Burges's work (1990a,b) which are related to soil moisture accounting model structure regarding the transitions from dry to wet catchment conditions and vice versa, as well as extreme rainfall. Thus, in Fig. 3, transitions from dry (small or zero

TABLE 8

Error analysis for 3-day volumes including peaks

444 peaks	Observed	Forecast
Mean 3-day volume	20.54	21.30
124 5.0 or less	2.56	3.74
161 others 20.0 or less	11.96	16.11
159 greater than 20.0	43.26	40.25
Mean peak-day flow	8.90	8.29
Day of 5-day discharge centroid	3.00	3.07

Standard error = 13.24.

(a)

year	month	day	PCP	OBS ($m^3/s/km^2$)	FCST ($m^3/s/km^2$)
1977	11	1	.00	.34	.17
		2	1.35	.34	.22
		3	1.30	.56	.59
		4	.00	.45	.68
		5	.00	.45	.32
		6	.00	.39	.19
		7	.00	.37	.19
		8	.00	.34	.18
		9	.00	.34	.18
		10	.00	.34	.17
		11	.00	.34	.17
		12	.00	.31	.16
		13	.00	.23	.16
		14	.01	.37	.15
		15	3.32	.67	2.31
		16	.30	.56	3.65
		17	5.30	4.03	6.45
		18	1.33	3.56	9.99
		19	2.72	3.32	9.19
		20	.75	1.77	7.28
		21	2.66	2.23	6.67
		22	.10	2.38	5.87
		23	.13	2.38	2.80
		24	.47	2.23	1.53
		25	.07	1.30	1.40
		26	.74	1.30	1.60
		27	2.71	3.34	4.54
		28	1.05	.98	7.11
		29	1.15	.83	6.32
		30	.84	1.30	4.85

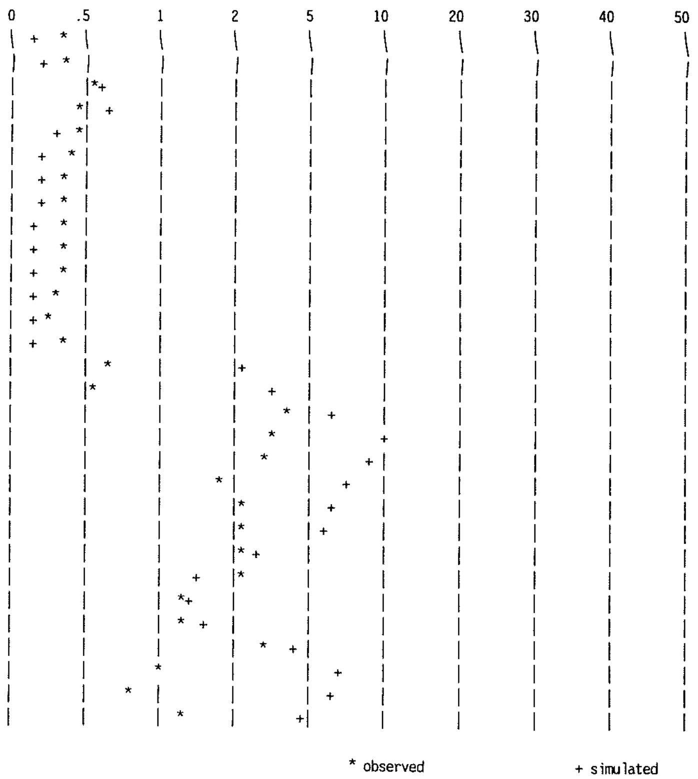

Fig. 3. Daily observed and simulated hydrographs for antecendent dry conditions.

values of rainfall) to wet (great values of rainfall) are presented. The simulated daily runoff from lightly underestimated values (comparable to observed values) shifted to apparently overestimated values.

For transitions from wet to dry conditions the simulated runoff values were close to the obsered ones (Fig. 4). In the case of extreme rainfall under dry antecedent conditions, the simulated runoff values were underestimated (Fig. 5). Yet when the antecendent conditions were wet, the extreme hydrograph response was best (Fig. 6). Despite the above discussed incompatibilities between daily simulated and observed runoff, the rainfall-runoff model reproduced successfully the monthly runoff, just as described in the previous section (model calibration).

Model verification

The plot of the long-term annual mean catchment pseudo-precipitation (rain plus melt) (Fig. 7) reflected three distinct periods with different climate

(b)

year	month	day	PCP	OBS (m3/s/km2)	FCST (m3/s/km2)
1979	10	1	.00	.27	.37
		2	1.30	.33	.42
		3	2.17	.55	.52
		4	1.74	.35	1.21
		5	.07	.32	1.39
		6	.00	.53	.67
		7	1.04	.70	.63
		8	.83	.73	1.12
		9	.05	.77	1.06
		10	.00	.63	.59
		11	.00	.63	.43
		12	.00	.58	.41
		13	.00	.58	.40
		14	.00	.53	.39
		15	.00	.53	.37
		16	.00	.53	.36
		17	.00	.48	.35
		18	.00	.48	.34
		19	1.42	.53	.40
		20	1.55	.53	1.29
		21	1.95	.63	3.28
		22	.56	.48	3.61
		23	.00	.48	1.84
		24	.00	.48	.70
		25	.12	.48	.49
		26	.45	.48	.49
		27	.19	.48	.47
		28	.58	.29	.77
		29	1.35	.61	1.98
		30	1.36	1.11	3.39
		31	5.51	3.05	7.95

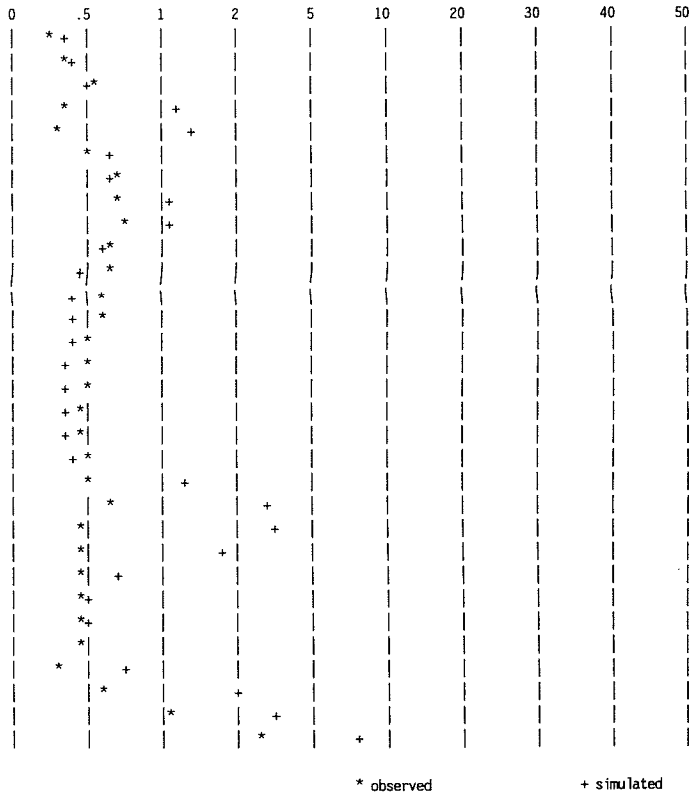

Fig. 3. Continued.

conditions. A modified differential split sample test was implemented in order to verify the ability of the model to respond, without significant deviation, to the three different climate periods. The model was run for each period separately, and the statistical variables: long-term annual mean runoff, standard deviation of annual runoff, and correlation coefficient of monthly runoff, were computed (Table 9). The null hypothesis H_0 of the variable difference between two climate periods and any climate period and calibration period was tested. The results for all variables fell within 95% of the critical region.

RESULTS

Because the snowmelt and soil moisture accounting models operate on daily or shorter time steps, and the models were run for 15 years, large amounts of computer output were generated. To simplify the analysis of results, we selected the following model (simulated) variables to describe the

(a)

year	month	day	PCP	OBS ($m^3/s/km^2$)	FCST ($m^3/s/km^2$)
1978	6	1	.70	3.40	2.67
		2	.52	3.28	2.59
		3	.62	3.28	2.50
		4	.85	3.28	2.44
		5	.19	2.91	2.37
		6	.01	2.91	2.27
		7	.12	2.31	2.18
		8	.03	2.31	2.12
		9	.01	2.31	2.06
		10	.00	2.20	2.01
		11	.00	2.06	1.96
		12	.00	2.01	1.92
		13	.00	2.01	1.88
		14	.00	1.84	1.84
		15	.00	1.84	1.81
		16	.00	1.32	1.77
		17	.00	1.28	1.74
		18	.00	1.19	1.71
		19	.00	1.11	1.68
		20	.00	1.11	1.65
		21	.00	1.08	1.62
		22	.00	1.01	1.60
		23	.00	1.01	1.57
		24	.00	.92	1.55
		25	.00	.92	1.52
		26	.00	.88	1.50
		27	.02	1.32	1.47
		28	.00	.94	1.45
		29	.00	.94	1.43
		30	.00	.94	1.41

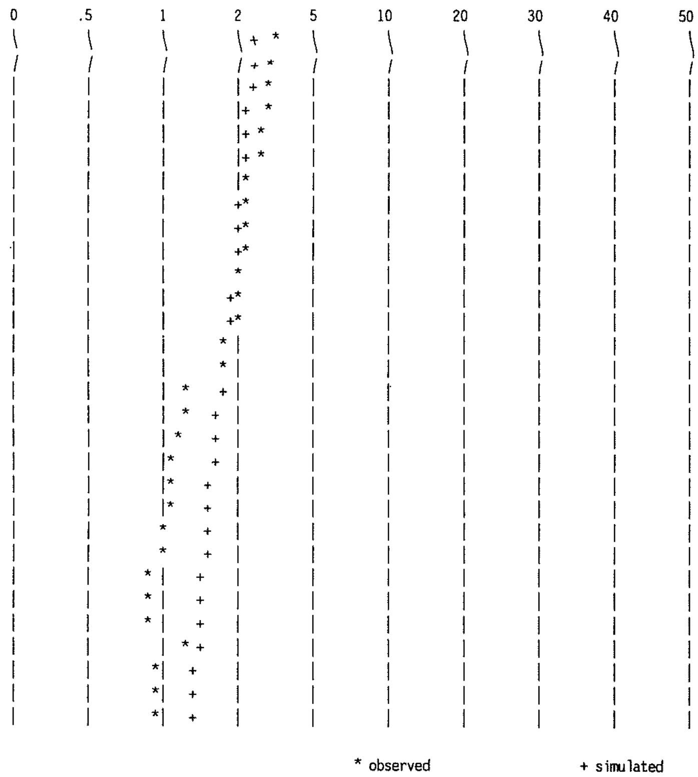

Fig. 4. Daily observed and simulated hydrographs for antecedent wet conditions.

TABLE 9

Values of statistical variables for climate periods and calibration period

Mesochora catchment pseudoprecipitation period	Annual runoff		Monthly runoff	
	Average value (cm)	Standard deviation (cm)	Standard error (cm)	Correlation coefficient
Intense descending	99.67	27.80	2.213	0.944
Intense rising	128.32	45.63	2.940	0.961
Mild descending	113.43	21.16	2.989	0.935
Calibration period	119.23	30.16	2.581	0.954

(b)

year	month	day	PCP	OBS	FCST
				$m^3/s/km^2$	
1980	12	1	3.79	25.13	28.41
		2	3.69	24.03	28.95
		3	1.98	21.50	25.80
		4	.87	16.28	19.94
		5	2.69	11.07	16.45
		6	.65	10.62	15.80
		7	1.51	15.97	14.10
		8	3.65	31.77	16.32
		9	.38	22.92	18.41
		10	.16	15.25	13.56
		11	.17	9.55	8.16
		12	.21	7.12	6.34
		13	.20	5.68	5.78
		14	.15	4.70	5.18
		15	.15	4.07	4.86
		16	.14	2.74	4.60
		17	.09	3.81	4.33
		18	.07	3.81	3.93
		19	1.53	4.07	5.79
		20	2.36	9.33	10.82
		21	2.20	9.74	15.35
		22	5.50	25.13	21.68
		23	2.07	18.81	27.41
		24	.25	15.97	22.98
		25	.04	8.19	13.36
		26	.03	7.80	7.53
		27	.02	7.29	5.61
		28	1.04	7.67	6.57
		29	.13	7.04	7.55
		30	.03	6.33	6.04
		31	.00	5.61	4.70

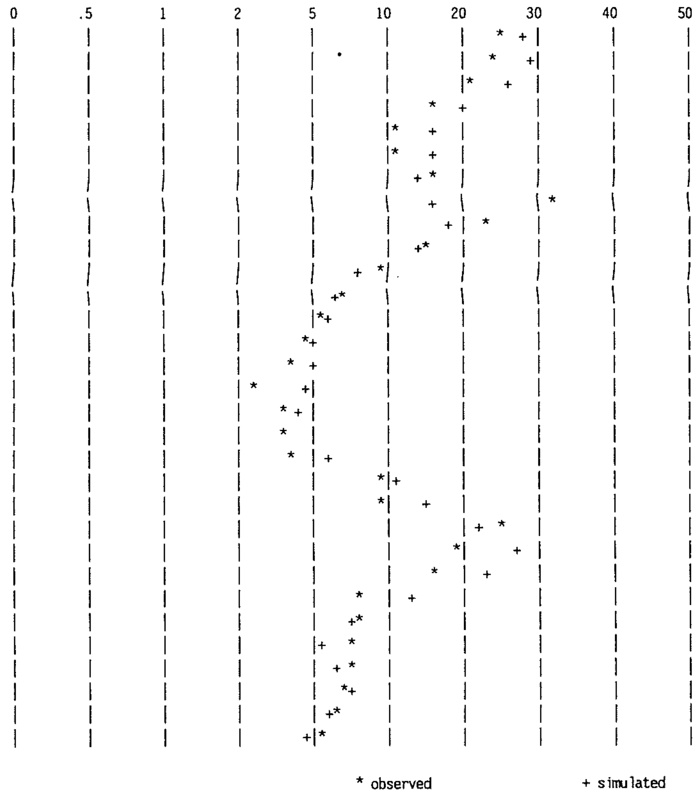

Fig. 4. Continued.

hydrological response of the catchment: (1) monthly mean weighted snow water equivalent over the catchment; (2) monthly mean catchment runoff; (3) monthly mean catchment evapotranspiration; (4) monthly mean catchment soil moisture storage in model zones.

Snow water equivalent

The catchment snow water equivalent by month resulted from the averaging of the snow water equivalent for the three elevation zones according to the ratios of the zone subareas to the total catchment area. The long term average catchment monthly snow water equivalent is plotted in Fig. 8.

Figure 8 shows that the hydrology of the Mesochora catchment is dominated by snow accumulation in winter and snowmelt in spring months with the largest mean snow water equivalent in March. Snow water storage is especially important because of the disproportionate amount of the precipitation that occurs at high elevations, and because snow water storage shifts

(a)

year	month	day	PCP	OBS	FCST
				m³/s/km²	
1974	10	1	.36	.36	.79
		2	.56	.36	.77
		3	.05	.36	.72
		4	.00	.33	.65
		5	.00	.33	.61
		6	.00	.50	.58
		7	.23	.31	.56
		8	3.27	.33	2.37
		9	.80	.33	3.90
		10	2.66	.47	4.77
		11	.26	.36	4.74
		12	.00	.28	2.29
		13	.00	1.25	.92
		14	1.01	.60	1.04
		15	.63	1.51	1.50
		16	5.93	10.79	6.86
		17	.00	6.24	10.70
		18	.00	2.07	5.86
		19	.00	.74	1.72
		20	.00	1.57	.89
		21	2.00	1.14	2.07
		22	9.01	45.14	11.82
		23	2.37	31.75	21.30
		24	.04	11.64	15.59
		25	.00	6.60	5.65
		26	.00	5.41	1.74
		27	.01	2.16	1.18
		28	.16	1.85	1.10
		29	.55	1.73	1.06
		30	4.52	4.91	5.78
		31	3.23	13.04	13.62

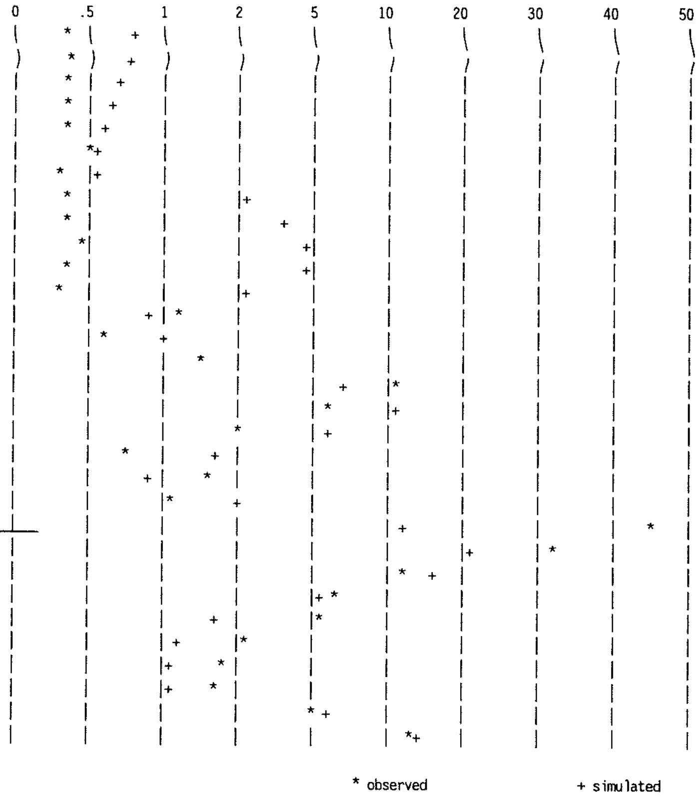

Fig. 5. Daily observed and simulated maximum runoff for antecedent dry conditions.

the peak of the annual runoff hydrograph from the high precipitation winter months toward the spring.

Runoff

The simulated and observed mean monthly runoff are also plotted in Fig. 8. Figure 8 shows that the mean monthly simulated runoff is very close to the observed one through all months, with simulation errors within the permitted limits. We note that the simulation error in February and March is 9.3% and 8.4% of the observed error, respectively.

The largest long-term average monthly runoff occurs in April and is the effect of March snow storage and melting. The monthly distribution of runoff and its variability are very important for water resources management.

(b)

$m^3/s/km^2$

year	month	day	PCP	OBS	FCST
1978	12	1	1.32	2.11	7.01
		2	.28	2.11	4.46
		3	.09	1.90	2.09
		4	.03	2.20	.94
		5	1.40	2.31	2.17
		6	.24	2.31	3.18
		7	.11	2.20	1.90
		8	.13	2.20	.94
		9	.12	2.20	.76
		10	.82	2.49	1.62
		11	.15	2.44	2.04
		12	.15	2.91	1.19
		13	.90	2.91	1.80
		14	2.08	4.60	4.54
		15	9.04	67.17	14.95
		16	.86	10.75	23.16
		17	.39	6.71	16.11
		18	.28	7.40	6.92
		19	.21	6.71	3.43
		20	.84	6.71	3.54
		21	.32	6.53	4.21
		22	.34	5.55	3.77
		23	1.13	4.78	4.47
		24	1.96	6.04	7.38
		25	.15	5.30	8.09
		26	.23	6.20	5.55
		27	2.84	12.03	7.15
		28	.26	9.11	9.88
		29	1.12	8.90	8.76
		30	.44	9.11	7.28
		31	.24	8.90	5.58

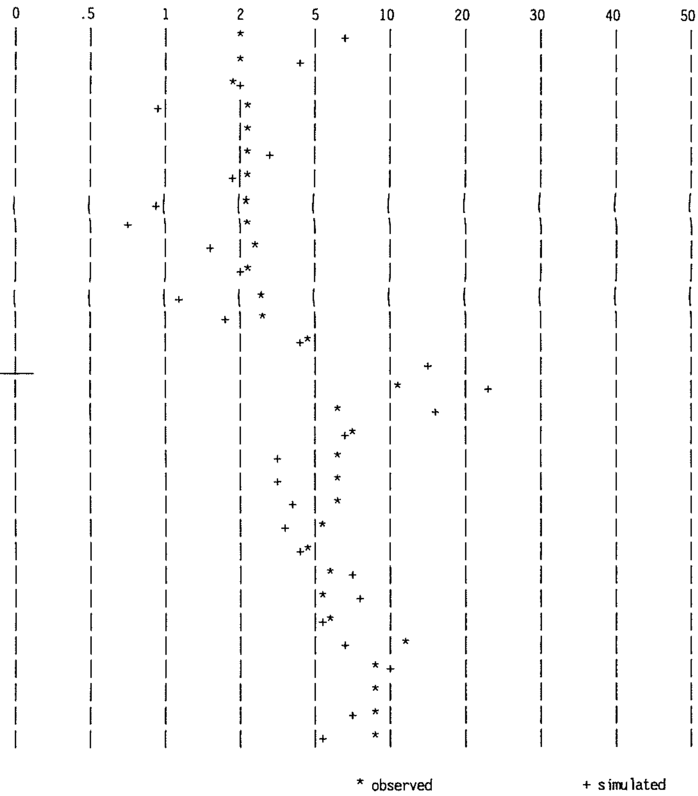

Fig. 5. Continued.

Evapotranspiration

The long-term average monthly catchment evapotranspiration is plotted in Fig. 8. The soil moisture accounting model assumes that the evapotranspiration depends on the moisture contents of the conceptual tension zones. The rate of evapotranspiration declines as the soil dries. Therefore, the shift of the flow from spring to winter affects the evapotranspiration accordingly. Evapotranspiration also depends upon temperature, meaning that wet winter soils do not yield as much evapotranspiration as similarly wet spring soils.

Soil moisture storage

Figure 8 and 9 graphically diplay the long-term average catchment soil moisture storages by month. The soil moisture accounting model has five conceptual storage zones.

The capacities and contents of the soil moisture zone were estimated from

(a)

year	month	day	PCP	OBS (m³/s/km²)	FCST (m³/s/km²)
1979	11	1	.40	2.77	10.43
		2	.09	2.77	5.55
		3	.74	2.17	2.13
		4	2.02	3.36	3.55
		5	2.27	3.61	6.59
		6	1.89	8.82	8.18
		7	.44	8.43	6.49
		8	.10	5.35	3.10
		9	.08	3.47	1.25
		10	.08	2.98	.88
		11	.09	4.56	.82
		12	2.78	8.82	3.63
		13	.46	5.35	6.15
		14	.12	3.47	3.85
		15	.64	3.88	2.03
		16	.83	3.20	2.67
		17	4.08	11.46	6.88
		18	.93	10.31	10.49
		19	5.68	13.18	13.52
		20	1.22	12.20	16.97
		21	.68	6.45	13.10
		22	.36	6.25	7.14
		23	.19	6.06	3.95
		24	.35	6.06	3.12
		25	2.21	5.22	5.69
		26	.44	4.48	8.08
		27	.12	3.05	6.00
		28	.03	2.36	3.31
		29	.02	2.36	2.35
		30	.05	2.36	2.09

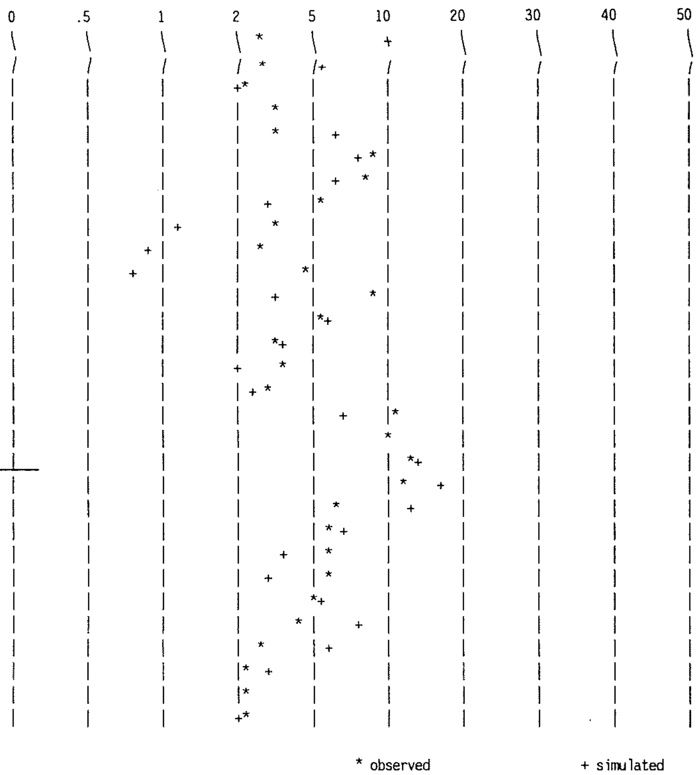

Fig. 6. Daily observed and simulated maximum runoff for antecedent wet conditions.

real determinative facts, while possible refinements were made through a trial and error approach. The absence of an automatic calibration and optimization procedure ensures that all model soil moisture storages reflect the physical soil moisture storage capacities of the catchment. However, there is no way to check the simulated soil moisture storages against actual soil moisture storages.

Figure 8 shows that the minimum tension moisture of the upper zone occurs in August, while the tension moisture of the lower zone reaches its minimum in October, reflecting the fact that several flora species can draw, during summer months, soil moisture from the lower tension moisture storage.

The upper free water zone (Fig. 9) reflects larger fluctuations in seasonal moisture distribution than the lower zones.

(b)

year	month	day	PCP	OBS ($m^3/s/km^2$)	FCST ($m^3/s/km^2$)
1982	11	1	.00	.94	.47
		2	.00	.80	.46
		3	.00	.73	.44
		4	.18	.65	.44
		5	.36	.73	.45
		6	.22	.73	.44
		7	1.15	.82	1.28
		8	.15	.65	1.61
		9	.10	.65	.78
		10	.06	.60	.46
		11	.03	.60	.44
		12	.01	.55	.42
		13	.01	.73	.41
		14	.09	1.93	.40
		15	3.75	4.75	3.97
		16	5.70	12.49	12.67
		17	10.02	21.97	25.53
		18	4.55	18.81	34.40
		19	.70	15.79	28.14
		20	.12	11.13	14.20
		21	.07	7.27	5.65
		22	.03	4.46	3.17
		23	.06	4.03	2.67
		24	.24	3.53	2.44
		25	.04	3.53	2.45
		26	.03	3.15	2.36
		27	.24	3.15	2.04
		28	1.11	3.42	3.59
		29	1.69	5.17	6.95
		30	2.07	9.31	10.04

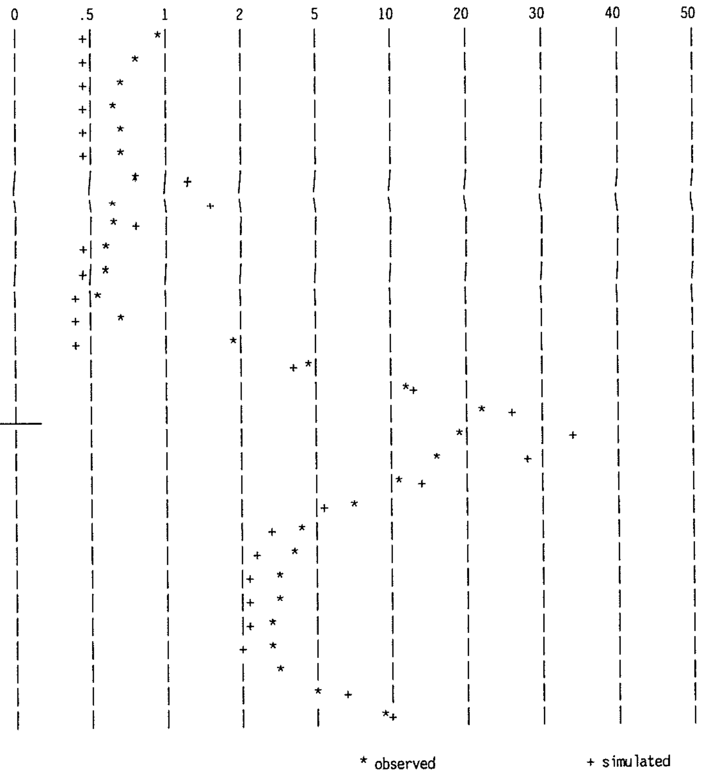

Fig. 6. Continued.

CONCLUSIONS

In this study, the hyrological modelling of a medium-size mountainous catchment from incomplete meteorological records was attempted. In order to preserve the physical meaning of model inputs and obtain a more accurate areal and elevation integration of the daily precipitation and temperature data, these latter were averaged by introducing a combinatorial technique of the Thiessen method and station availability condition. The snow accumulation and ablation model, as well as the soil moisture accounting model of US NWS, were used for the dynamics simulation of the catchment under study.

By using the aforesaid input modelling, the snowmelt model proved capable of predicting the initiation of snow accumulation in the fall and the gradual melting of the snowpack in the late winter and spring. The second model also proved capable of exactly reproducing both the magnitude and timing of annual and monthly runoff, as well as estimating evapotranspiration and soil moisture storages. On a daily basis, the soil moisture model

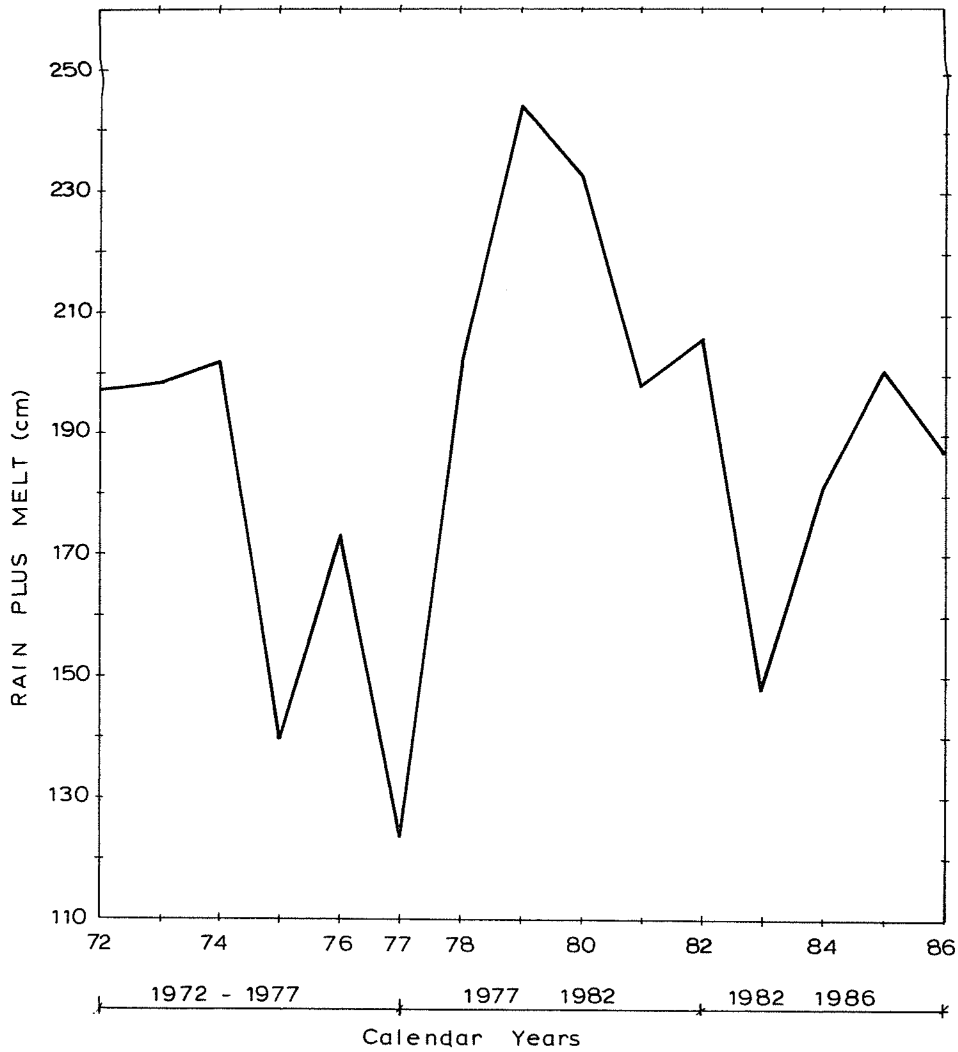

Fig. 7. Annual pseudoprecipitation (rain plus melt) of the Mesochora catchment.

reproduced, satisfactorily, the historic data, while some discrepancies were pointed out for the following characteristic conditions:

(1) during transitions from dry to wet conditions the simulated streamflow values were overestimated in comparison with the observed ones;

(2) for especially extreme rainfall the reproduction of hydrological response was rather unreliable.

These discrepancies are the same as those of Gan and Burges and for the

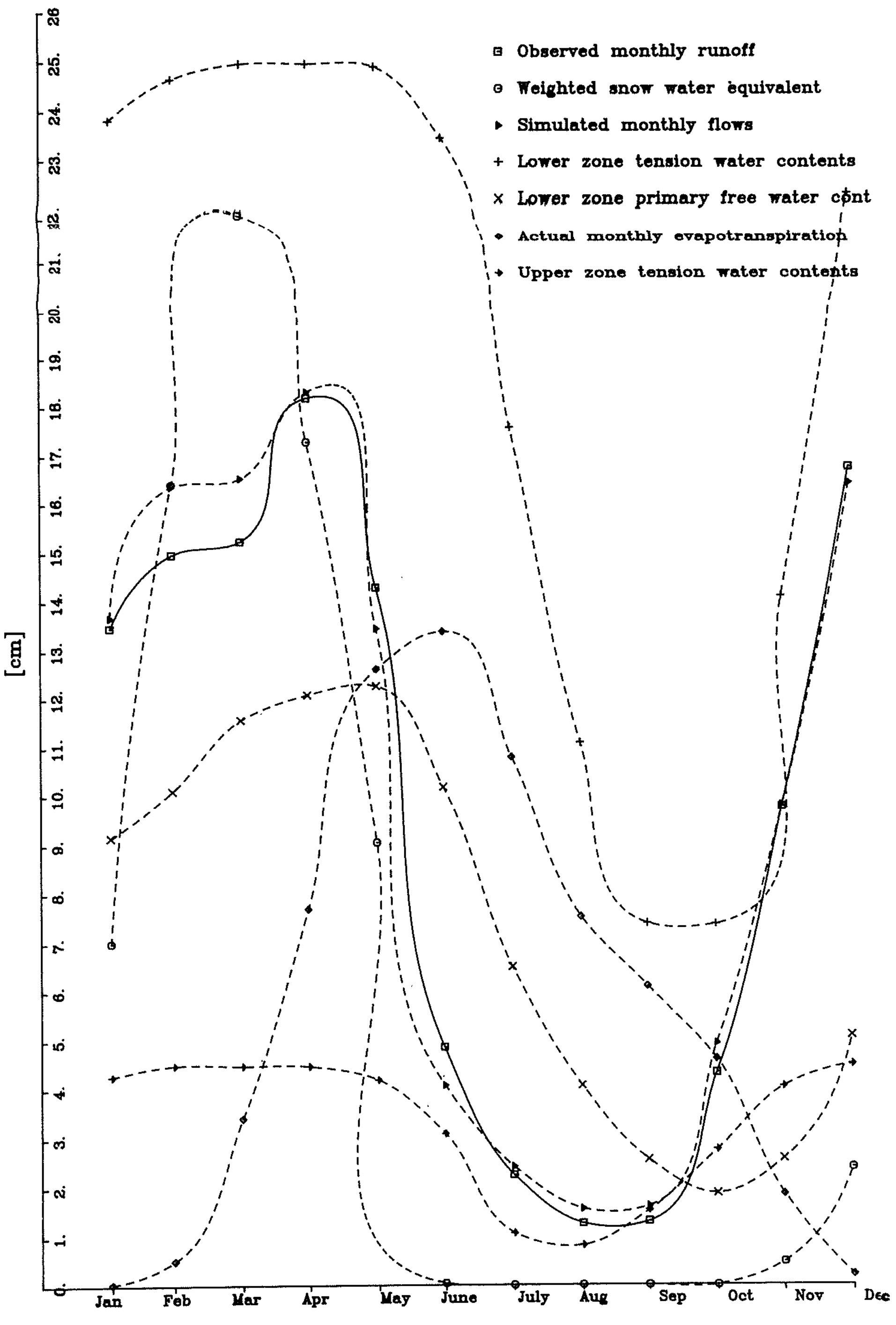

Fig. 8. The Mesochora catchment observed and simulated runoff, weighted snow water equivalent, evapotranspiration, lower zone tension water contents, lower zone primary free water contents and upper zone tension water contents (mean monthly values).

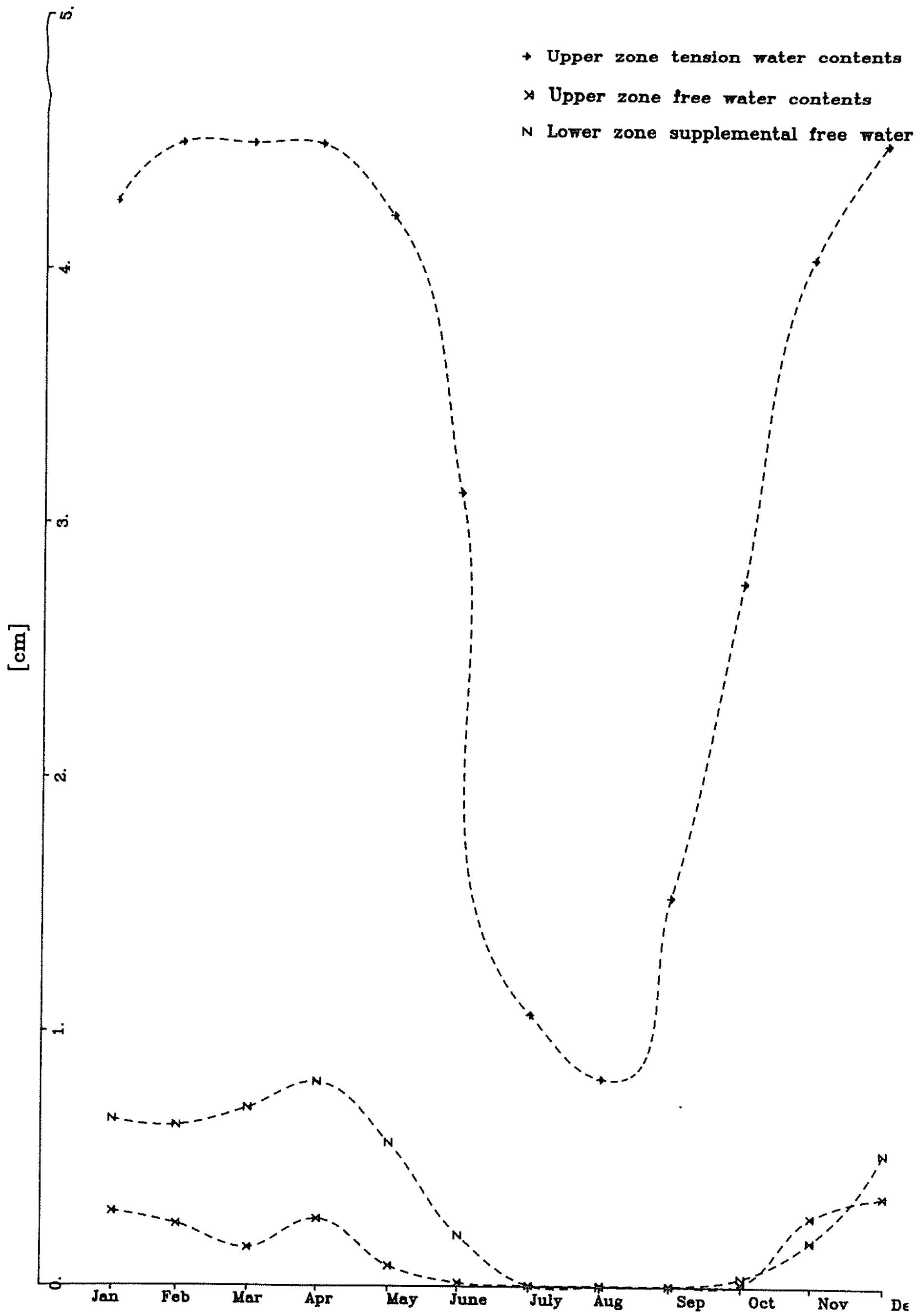

Fig. 9. The Mesochora catchment mean monthly upper zone tension water contents, upper zone free water contents and lower zone supplemental free water contents.

present study they are related rather to soil moisture model structure than to rainfall modelling which was as far as possible free from simulation errors. For this reason, the time scale that is used for hydrological response analysis of climate change (the most serious problem in our century) by using the US NWS soil moisture model, has a great significance for obtaining more accurate results. Keeping fully in mind this time horizon, we used a long-average monthly scale for the hydrological analysis of hypothetical climate change scenarios (Panagoulia, 1991b), as well as those scenarios relating to the GISS (NASA) general circulation model (Panagoulia, 1992).

ACKNOWLEDGEMENTS

We wish to extend our sincere thanks to the president of IAHS Vit Klemes for supplying us with his article entitled 'The Modelling of a Mountain Hydrology: The Ultimate Challenge' from which many aspects have fed our Introduction.

Also, we thank sincerely the civil engineer George Dimou who helped us on computer themes.

REFERENCES

Anderson, E.A., 1973. National Weather Service River Forecast System – snow accumulation and ablation model. NOAA Technical Memorandum NWS HYDRO-17. National Oceanic and Atmospheric Administration, Silver Spring, MD.

Burnash, R.J.C., Ferral, R.L. and Mcquire, R.A., 1973. A generalized streamflow simulation system conceptual modelling for digital computers. US National Weather Service, Sacramento, CA, 203 pp.

Crawford, N.H. and Linsley, R.K., 1966. Digital simulation in hydrology: Stanford Watershed Model IV, Stanford University, Department of Civil Engineering Technical Report 39.

Gan, T.Y. and Burges, S.J., 1990a. An assessment of a conceptual rainfall–runoff model's ability to represent the dynamics of small hypothetical catchments. 1. Models, model properties, and experimental design. Water Resour. Res., 26(7): 1595–1604.

Gan, T.Y. and Burges, S.J., 1990b. An assessment of a conceptual rainfall–runoff model's ability to represent the dynamics of small hypothetical catchments. 2. Hydrologic responses for normal and extreme rainfall. Water. Resour. Res., 26(7): 1605–1619.

Huggins, L.F. and Burney, J.R., 1982. Surface runoff storage and routing. In: C.T. Haan, H.P. Johnson and D.P. Brakensiek (Editors), ASAE Monograph No. 5: Hydrologic modelling of Small Watersheds, pp. 169–225

James, L.D. and Burges, S.J., 1982. Selection, calibration, and testing of hydrologic models. In: C.T. Haan, H.P. Johnson and D.P. Brakensiek (Editors), ASAE Monograph No. 5: Hydrologic Modeling of Small Watersheds, pp. 437–472.

James, L.D., Bowels, D.S. and Hawkins, R.H., 1982. A taxonomy for evaluating surface water quantity model reliability. International Symposium on Rainfall–Runoff Modelling, May 18–21. Mississippi State University, Mississippi State, MS.

Jamienson, D.G. and Wilkinson, J.C., 1972. Operating multi-purpose reservoirs for water supply and flood alleviation. Water Resour. Res., 8: 899–903.

Klemes, V., 1990. The modelling of mountain hydrology. The ultimate challenge. In: I. Molnar (Editor), Hydrology of Mountainous Areas. IAHS Publ., No. 190, pp. 29–43.

Linsley, R.K., 1982. Rainfall–runoff models. In: V.P. Singh (Editor), An Overview in Rainfall–Runoff Relationship, Water Resour. Publ., pp. Littleton, CO., 3–22.

Linsley, R.K., Kohler, Max A. and Paulhus, J.L.H., 1988. Hydrology for Engineers, McGraw-Hill, NY.

Panagoulia, D., 1990. Sensitivity analysis of catchment hydrological response to climate changes. Ph.D. Thesis. National Technical University of Athens.

Panagoulia, D., 1991a. A technique estimating daily catchment precipitation with elevation correction for conceptual simulation. Proceedings of European Conference Advances in Water Resources Technology, 89–101, A.A. Balkema, G. Tsakiris (Editor), Athens, 20–23 March.

Panagoulia, D., 1991b. Hydrological response of a medium-sized mountainous catchment to climate changes. Hydrol. Sci. J., 36(6): 525–547.

Panagoulia, D., 1992. Impacts of GISS-modelled climate changes on catchment hydrology. Hydrol. Sci. J., in press.

Peck, E.L., 1976. Catchment modelling and initial parameter estimation for the National Weather Service Forecast System. NOAA Techn. Memorandum NWS HYDRO 31, National Oceanic and Atmospheric Administration, Washington, DC.

Schermerhorn, V.P. and Kuehl, D.W., 1968. Operational streamflow forecasting with the SSARR model. Int. Assoc. Sci. Hydrol. Publ., 80: 317–328.

Shaw, E.M., 1984. Hydrology in Practice. Van Nostrand Reinhold UK Berkshire, UK.

U.S. Agricultural Research Service, 1975. US DAHL-74, revised model for watershed hydrology. Tech. Bull., 158.

Veihmeyer, F.J., 1964. Evapotranspiration. In: Chow Handbook of Applied Hydrology McGraw-Hill NY.

Woolhiser, D.A. and Brakensiek, D.L., 1982. Hydrologic system synthesis. In: C.T. Haan, H.P. Johnson and D.L. Brakensiek (Editors), ASAE Monograph No. 5: Hydrologic modelling of small watersheds, pp. 3–10.

World Meterological Organization, 1975. Intercomparison of conceptual models used in operational hydrological forecasting, World Meteorological Organization, Geneva, Operational Hydrology Report No 7, Annex III, 47 pp.

World Meteorological Organization, 1986. Intercomparison of snowmelt runoff. World Meteorological Organization, Geneva, Operational Hydrology Report No. 23, pp. 65–75.